

## Supporting Information

### Defect engineering within clusters to enhance cluster-support

#### interaction boosts catalytic performance

Jiankang Chen,<sup>‡a</sup> Yangping Wang,<sup>‡a</sup> Yu Zhang,<sup>‡a</sup> Huan Yan,<sup>b</sup> Qinzhen Li,<sup>a</sup> Jinsong Chai,<sup>a</sup> Guiqi Gao,<sup>\*a</sup> Chunyan Liu,<sup>\*b</sup> Sha Yang<sup>\*a</sup> and Manzhou Zhu<sup>a</sup>

<sup>a</sup> Institutes of Physical Science and Information Technology, Department of Chemistry and Centre for Atomic Engineering of Advanced Materials, Key Laboratory of Structure and Functional Regulation of Hybrid Materials of Ministry of Education, Anhui Province Key Laboratory of Chemistry for Inorganic/Organic Hybrid Functionalized Materials, Anhui University, Hefei, Anhui 230601, China

<sup>b</sup> College of Chemistry and Chemical Engineering, Hunan University, Changsha, Hunan 410082, China  
E-mail: gaoguiqi1@126.com (G.G.); cyliu@hnu.edu.cn (C.L.); yangshac@ahu.edu.cn (S.Y.)

<sup>‡</sup> J. C., Y. W., and Y. Z. contributed equally to this work.

## Experimental Procedures

### Materials.

All reagents were commercially available and used without further purification. Dichloromethane (DCM, HPLC grade), methanol (MeOH, HPLC grade), toluene (TOL, HPLC grade), n-hexane (Hex, HPLC grade), 4-tert-butylphenylthiophenol (TBBT,  $\geq 99\%$ ), activated carbon (AC), graphene (GR), carbon nanotubes (CNT), silica ( $\text{SiO}_2$ ), tetraoctylammonium bromide (TOAB,  $\geq 98\%$ ), tri(m-tolyl)phosphine (TPMP,  $\geq 98\%$ ),  $\text{HAuCl}_4 \cdot 4\text{H}_2\text{O}$  ( $\geq 99.99\%$ , metal basis), borane tert-butylamine complex ( $\text{C}_4\text{H}_{14}\text{BN}$ ,  $\geq 95\%$ ) were all purchased from Shanghai Aladdin Bio-ChemTechnology Co.

### Synthesis of $\text{Au}_{44}(\text{TBBT})_{28}$

$\text{Au}_{44}(\text{TBBT})_{28}$  was synthesized according to a previous report with some modifications.<sup>1</sup> Briefly, mix 400  $\mu\text{L}$  of  $\text{HAuCl}_4 \cdot 4\text{H}_2\text{O}$  (0.2 g/mL) with 100 mg of TOAB in 5 mL of MeOH and 10 mL of DCM. After 5 minutes, add 150  $\mu\text{L}$  of TBBT. After 10 minutes, directly add 120 mg of the borane-tert-butylamine complex. Stir at room temperature for 8 hours, then remove the solvent. The residue was washed with MeOH, and the crude product was dissolved in 2 mL of TOL, to which 100  $\mu\text{L}$  of TBBT was added. The etching process was carried out at 60 °C for 12 hours. Finally, the crude product was further purified on a thin-layer chromatography (TLC) plate (Hex : DCM = 3 : 1).

### Synthesis of $\text{Au}_{40}(\text{TBBT})_{24}(\text{TPMP})$

Dissolve 5 mg of  $\text{Au}_{44}(\text{TBBT})_{24}$  in 3 mL of toluene in a 50 mL round-bottom flask. Place the flask in a 60 °C oil bath. Then, dissolve 0.5 mg of tri(m-tolyl)phosphine in 0.5 mL of toluene and add it to the flask. Stir the mixture slowly for approximately 30 minutes. After that, the solution was concentrated with a rotary evaporator and precipitated with the addition of methanol. The precipitate was further washed twice with methanol. The raw product was separated using a thin-layer chromatography plate. It was found that  $\text{Au}_{44}$  was completely transformed, while  $\text{Au}_{40}$  was a brownish-green band.

### Measurement

The UV-vis absorption spectrum of the nanocluster solution in this work was obtained using a METASH UV-9000 spectrophotometer. The ESI-MS measurement was recorded using a Waters Xevo G2-XS Q Tof mass spectrometer. The morphologies of the catalysts were obtained using a JEM 2100 transmission electron microscope. XPS measurements were performed on a thermal ESCALAB 250, equipped with a monochromated Al  $K\alpha$  (1486.8 eV) 150 W X-ray source. The single-crystal structure of the nanocluster was obtained using a Stoe Stadivari Diffraction equipped with a digital camera diffractometer comprising a microfocus rotating anode X-ray source (Cu  $K\alpha$ ,  $\lambda = 1.54186 \text{ \AA}$ ).

### Preparation method of the catalyst

First, disperse activated carbon in dichloromethane, and then add nanoclusters (based on the mass of the clusters, with a mass fraction of 5% wt). The reaction mixture was stirred continuously for about 5 hours, and the solvent was removed by centrifugation. The samples were dried in a vacuum oven and used as catalysts directly without further treatment.

### Catalytic experiment

10 mg of the catalyst was added to 1 mL of 4-nitrophenol, and the mixture was stirred at room temperature for 10 minutes. Then, 1 mL of aqueous solution containing  $\text{NaBH}_4$  (0.53 mmol, 20 mg) was added to the mixture under continuous stirring. All catalytic reactions were carried out at room temperature. Monitored by an ultraviolet-visible adsorption spectrometer.

### Computational Details

All density functional theory calculations were performed using the Vienna Ab initio Simulation Package (VASP). The exchange-correlation energy was described by the Perdew-Burke-Ernzerhof (PBE)

functional within the generalized gradient approximation, supplemented with the DFT-D<sup>3</sup> method for van der Waals corrections. The projector-augmented plane wave (PAW) potentials were used to describe the core-valence electron interaction.

Geometry optimizations for the isolated Au<sub>n</sub> clusters (Au<sub>40</sub> and Au<sub>44</sub>) and their adsorption configurations on a graphene substrate were performed using a plane-wave energy cutoff of 450 eV. A cubic supercell with dimensions of approximately 40 × 40 × 40 Å<sup>3</sup> was used to ensure sufficient vacuum separation between periodic images. Given the large supercell size, the Brillouin zone was sampled solely at the  $\Gamma$ -point (a 1×1×1 k-point mesh). The conjugate gradient algorithm was used to relax all atomic positions until the forces on each atom were less than 0.03 eV/Å. The convergence threshold for electronic self-consistency was set to 10<sup>-4</sup> eV, with a Gaussian smearing width of  $\sigma = 0.05$  eV applied to the orbital occupation.

To quantify the interfacial charge transfer, Bader charge analysis was performed on the fully optimized structures. This required a set of high-precision, static single-point calculations with a tighter electronic convergence criterion of 10<sup>-7</sup> eV. For a visual analysis of charge redistribution at the interface, charge density difference ( $\Delta\rho$ ) maps were constructed according to the formula:

$$\Delta\rho = \rho_{\text{system}} - \rho_{\text{graphene}} - \rho_{\text{cluster}}$$

where  $\rho_{\text{system}}$  is the total charge density of the relaxed adsorption complex, and  $\rho_{\text{graphene}}$  and  $\rho_{\text{cluster}}$  are the charge densities of the isolated graphene substrate and the cluster, respectively, each fixed in the geometry they adopt within the composite system.

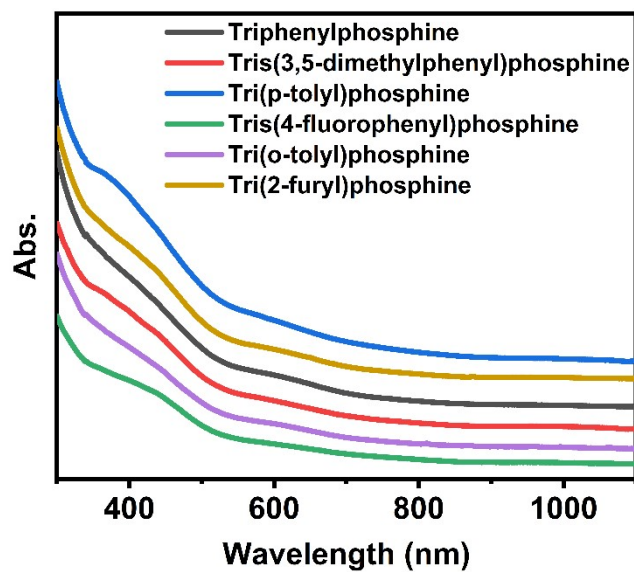


Fig. S1 UV-vis spectra of  $\text{Au}_{40}(\text{TBBT})_{24}(\text{PR}_3)$ . ( $\text{PR}_3$  = monophosphine)

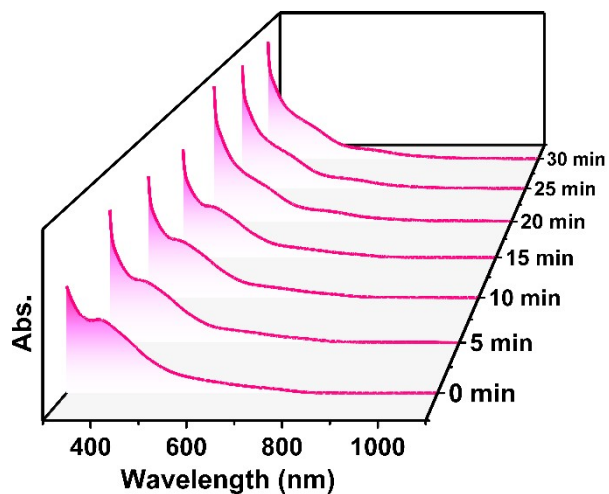


Fig. S2 Time-dependent UV-vis spectra of  $\text{Au}_{40}$  conversion process.

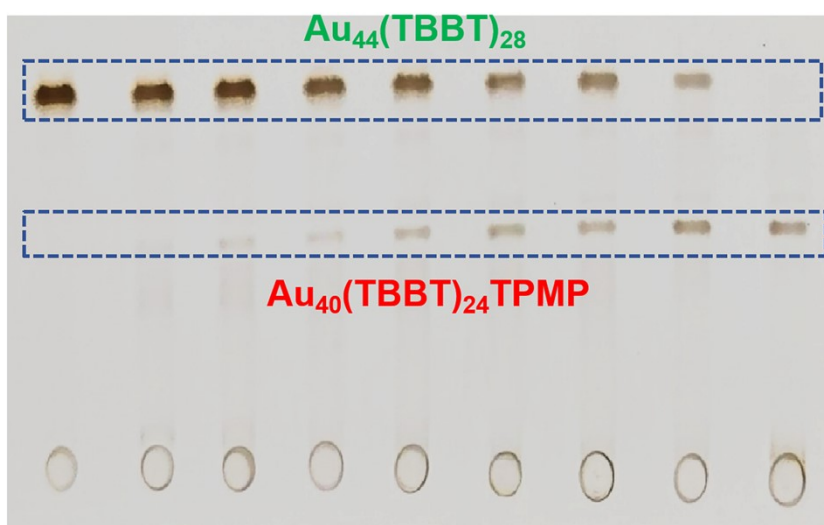
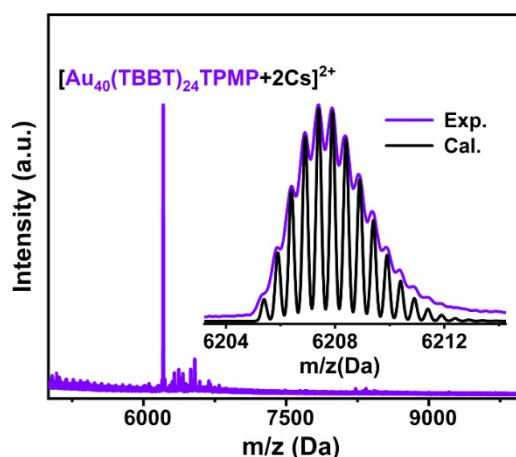


Fig. S3 TLC image of the conversion process.



**Fig. S4** ESI-MS spectrum of Au<sub>40</sub>.

**Table S1.** Crystal data and structure refinement for Au<sub>40</sub> cluster.

CCDC code	2496950
Empirical formula	C <sub>261</sub> H <sub>333</sub> Au <sub>40</sub> PS <sub>24</sub>
Formula weight	12149.32
Temperature/K	120
Crystal system	monoclinic
Space group	P2 <sub>1</sub> /c
a/Å	21.447
b/Å	28.586
c/Å	50.950
α/°	90
β/°	93.67
γ/°	90
Volume/Å <sup>3</sup>	31171.7
Z	4
ρ <sub>calc</sub> /cm <sup>3</sup>	2.589
μ/mm <sup>-1</sup>	36.223
F(000)	21832.0
Crystal size/mm <sup>3</sup>	0.34 × 0.16 × 0.07
Radiation	CuKα (λ = 1.54186)
2θ range for data collection/°	6.954 to 129.994
Index ranges	-25 ≤ h ≤ 10, -32 ≤ k ≤ 33, -57 ≤ l ≤ 59
Reflections collected	98817
Independent reflections	50114 [R <sub>int</sub> = 0.0786, R <sub>sigma</sub> = 0.1134]
Data/restraints/parameters	50114/1960/2676
Goodness-of-fit on F <sup>2</sup>	0.920
Final R indexes [I ≥ 2σ (I)]	R <sub>1</sub> = 0.0871, wR <sub>2</sub> = 0.2319
Final R indexes [all data]	R <sub>1</sub> = 0.1319, wR <sub>2</sub> = 0.2861
Largest diff. peak/hole / e Å <sup>-3</sup>	3.12/-3.91

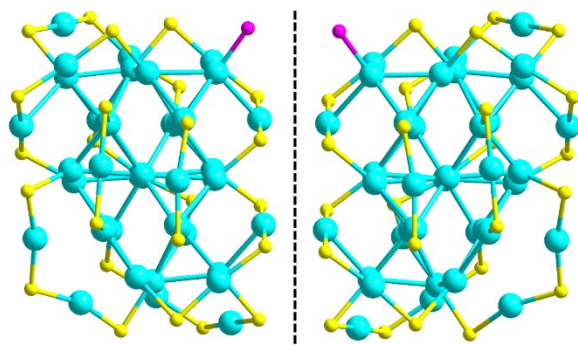


**Fig. S5** Core structures of the  $\text{Au}_{40}(\text{TBBT})_{24}(\text{TPMP})$  enantiomer pair. (Color label: Turquoise = Au, Yellow = S, Pink = P)

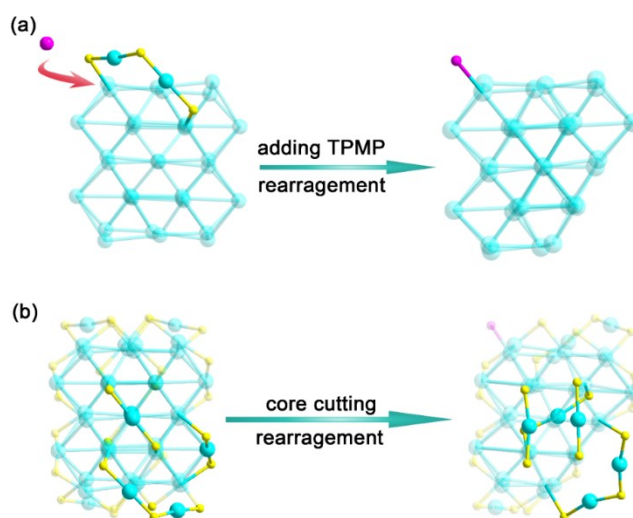


**Fig. S6** (a) Surface ligand rearrangement caused by phosphine ligands; (b) peripheral ligand rearrangement caused by the change of the kernel. (Color label: Turquoise = Au, Yellow = S, Pink = P)

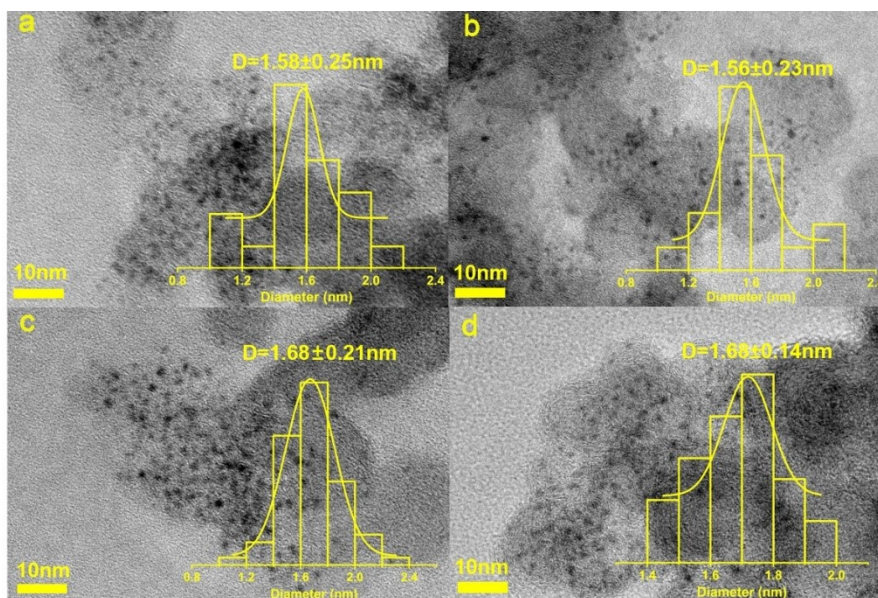


**Fig. S7** TEM images of the catalysts before (a)  $\text{Au}_{40}/\text{AC}$  and (b)  $\text{Au}_{44}/\text{AC}$ , and after (c)  $\text{Au}_{40}/\text{AC}$  and (d)  $\text{Au}_{44}/\text{AC}$  the reaction.

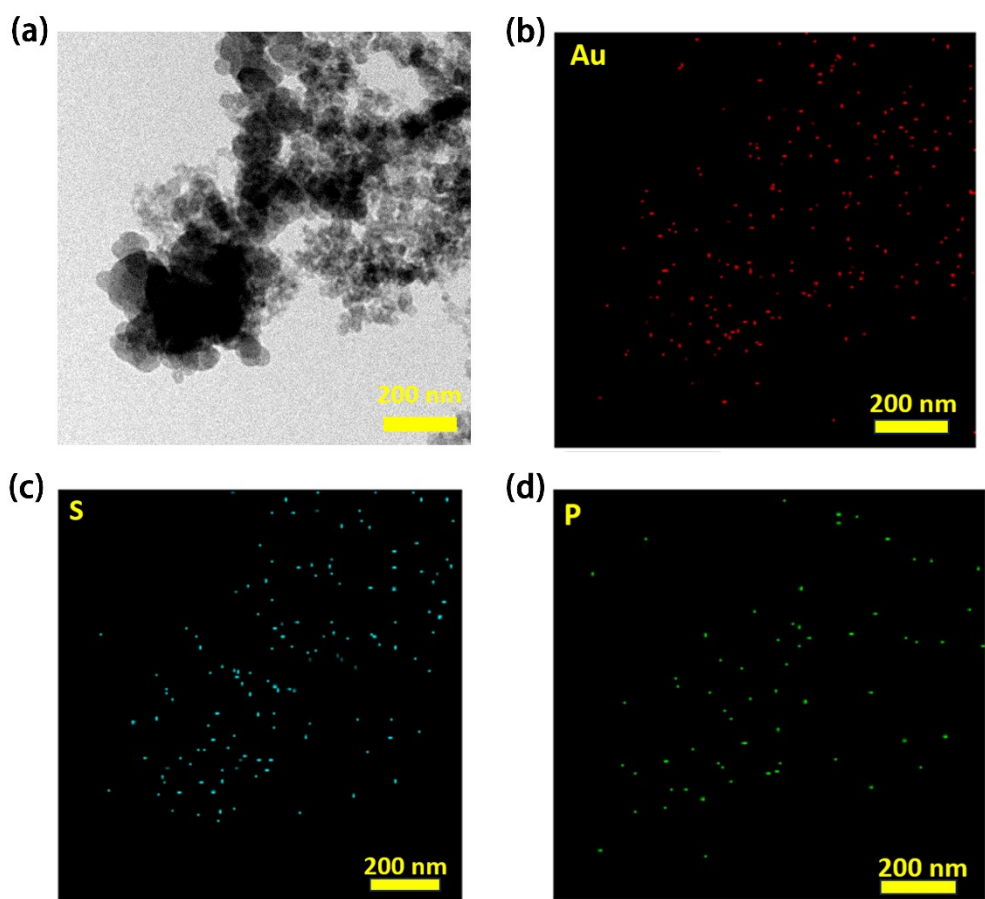


**Fig. S8** TEM Mapping elemental analysis for Au<sub>40</sub>/AC.

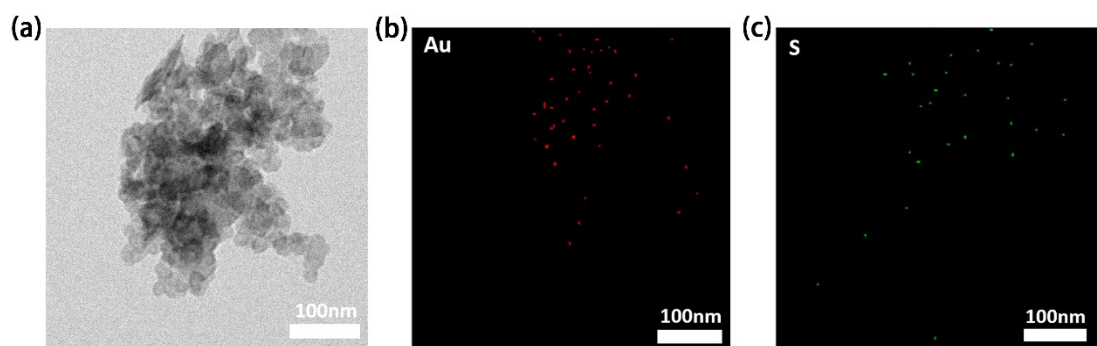


**Fig. S9** TEM Mapping elemental analysis for Au<sub>44</sub>/AC.

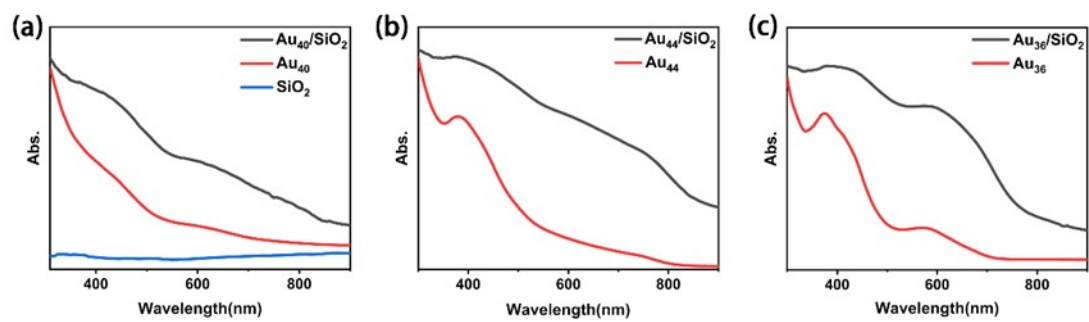


**Fig. S10** Solid-state UV-vis spectroscopy for (a) Au<sub>40</sub>; (b) Au<sub>44</sub>; (c) Au<sub>36</sub>.

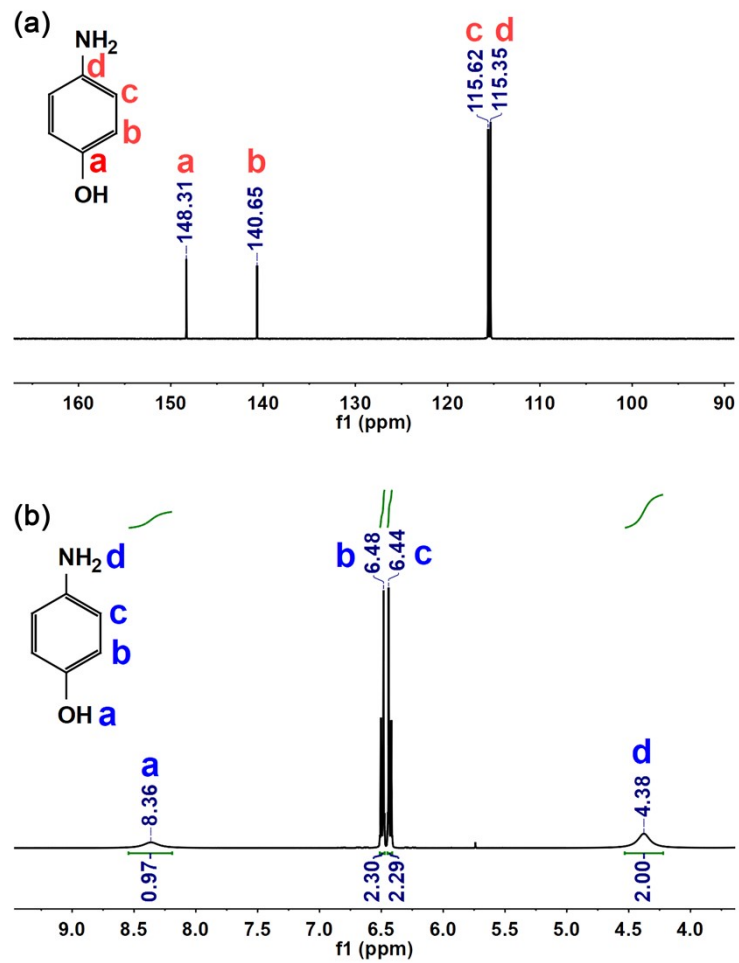


Fig. S11 The (a) <sup>13</sup>C NMR and (b) <sup>1</sup>H NMR spectra of 4-AP after catalysis dissolved in d<sub>6</sub>-DMSO.

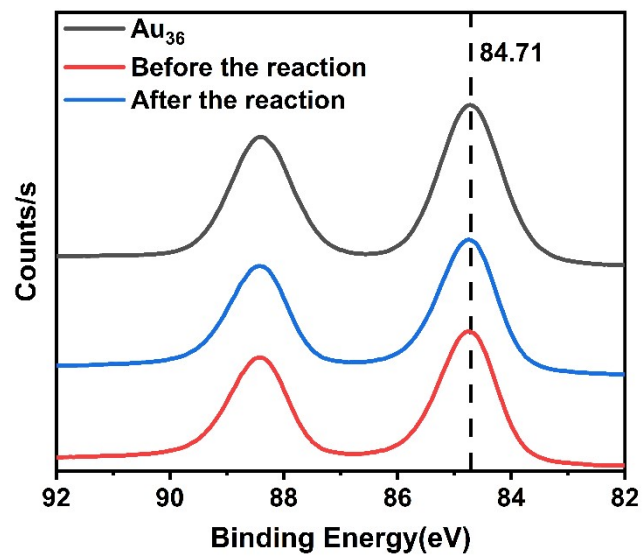
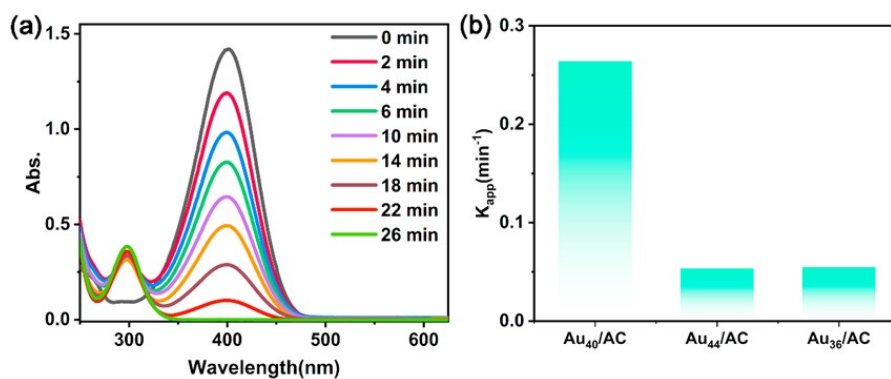
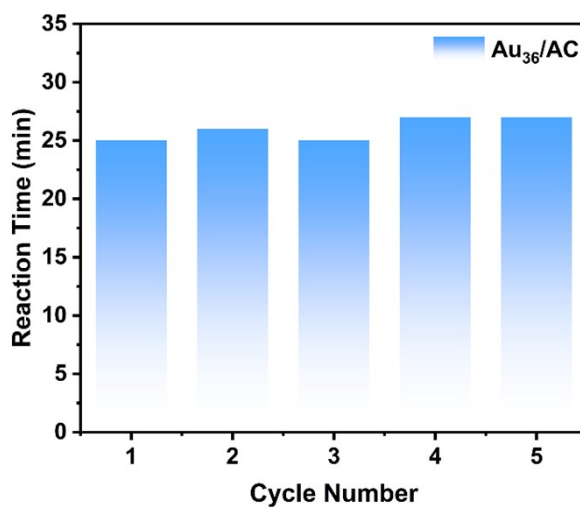


Fig. S12 Au<sub>36</sub> clusters on activated carbon before and after catalytic reaction.



**Fig. S13** (a) UV-vis spectra of reaction solution under catalysts of  $\text{Au}_{36}/\text{AC}$ . (b) Catalytic apparent rate constants ( $K_{\text{app}}$ ) of  $\text{Au}_{40}/\text{AC}$ ,  $\text{Au}_{44}/\text{AC}$  and  $\text{Au}_{36}/\text{AC}$ .



**Fig. S14** Complete degradation time of recycling catalytic experiments catalyzed with  $\text{Au}_{36}$  clusters.

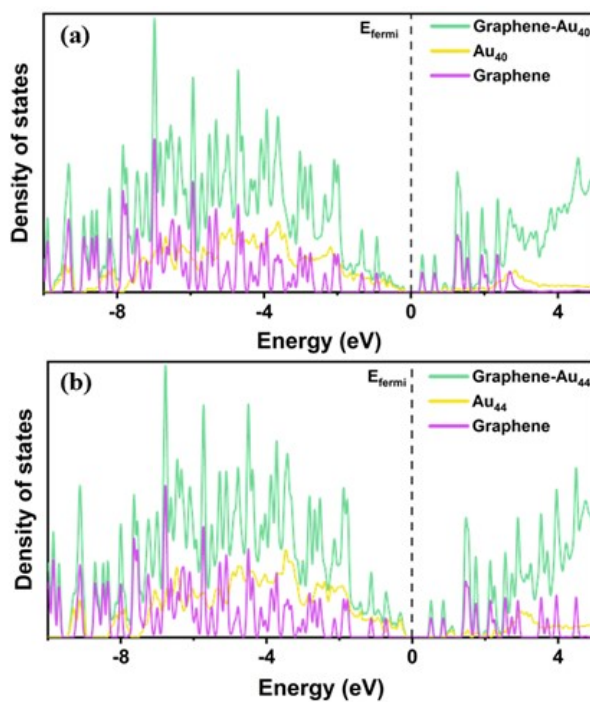


**Fig. S15** The PDOS of (a)  $\text{Au}_{40}$ -graphene and (b)  $\text{Au}_{44}$ -graphene.

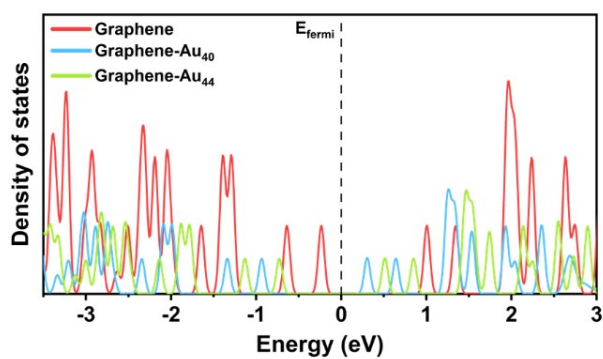


Fig. S16 The DOS of graphene in different system.

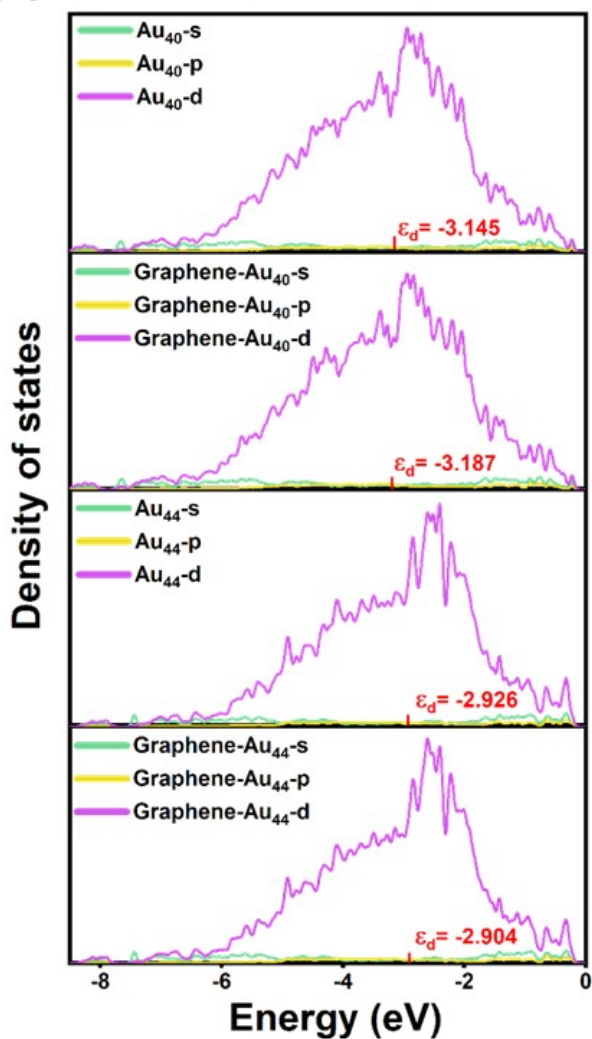


Fig. S17 The DOS of the cluster in different system.

Table S2. Energy of Au clusters before and after adsorption on graphene.

Cluster	Energy before adsorption (eV)	Energy after adsorption (eV)	$\Delta E$ (eV)
Au <sub>40</sub>	-3856.2495	-3856.2365	0.013
Au <sub>44</sub>	-4170.0184	-4170.0186	-0.0002

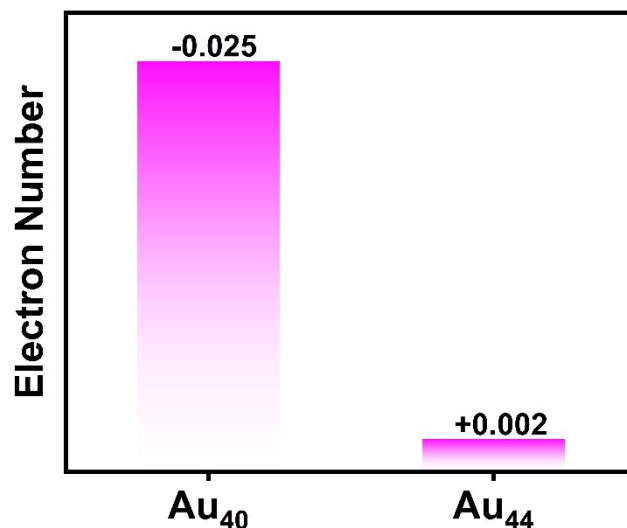


Fig. S18 Barder charge analysis of Au<sub>44</sub> and Au<sub>40</sub> cluster.

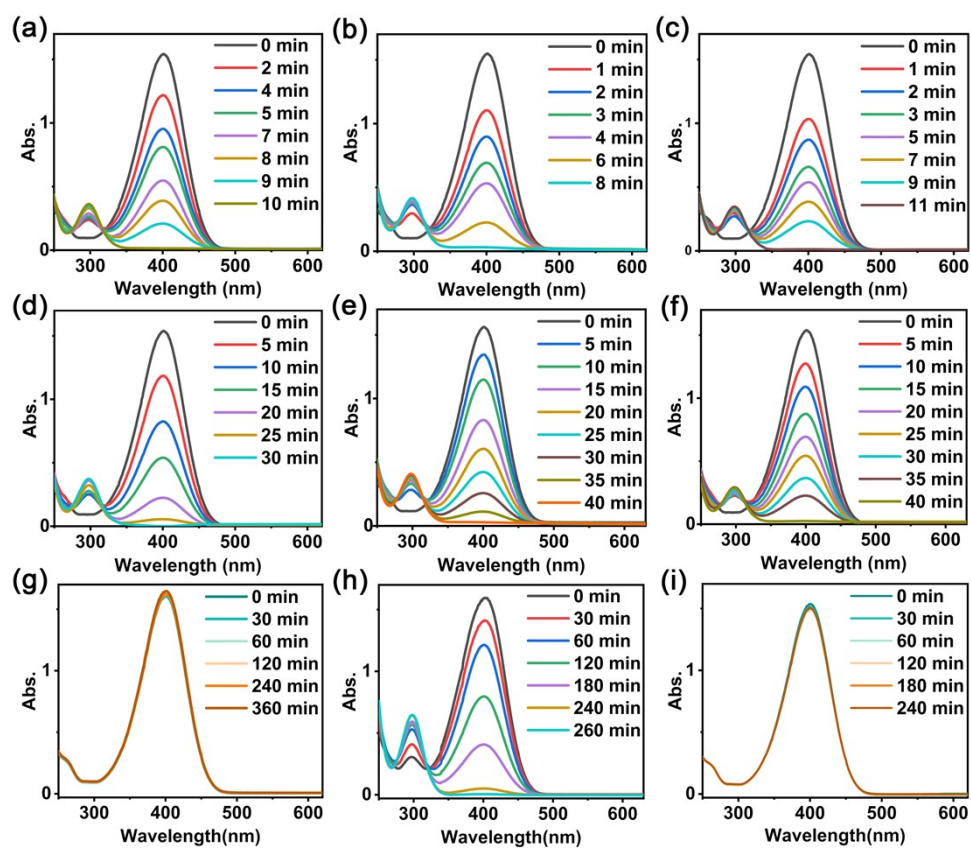


Fig. S19 UV-vis spectra showing gradual reduction of 4-nitrophenol catalyzed by different catalysts: (a-c) Au<sub>40</sub> nanocluster loaded on CNT, SiO<sub>2</sub> and GR, respectively; (d-f) Au<sub>44</sub> cluster loaded on CNT, SiO<sub>2</sub> and GR, respectively. (g) Au<sub>40</sub> cluster, (h) Au<sub>44</sub> cluster, and (i) AC.

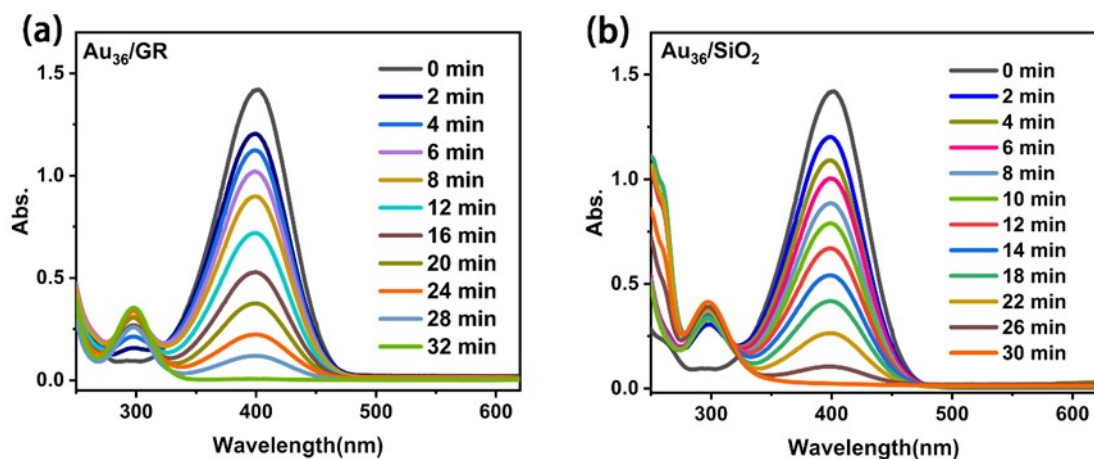


Fig. S20 UV-vis spectra of reaction solution under catalysts of (a)  $\text{Au}_{36}/\text{GR}$  and (b)  $\text{Au}_{36}/\text{SiO}_2$ .

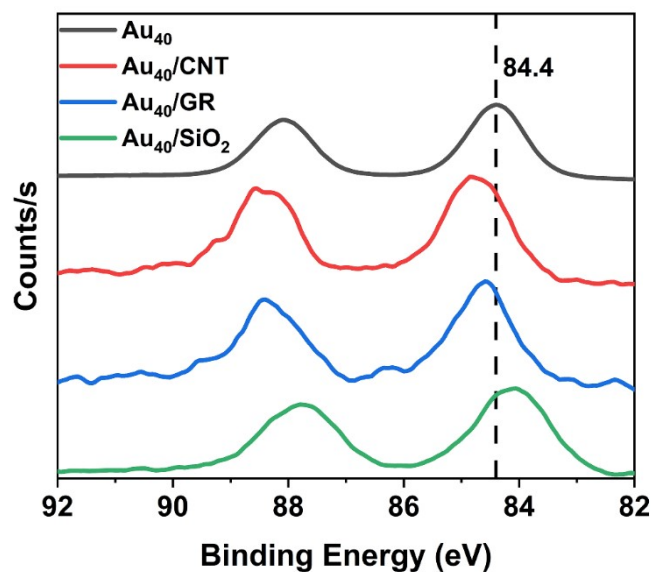


Fig. S21 XPS spectra of  $\text{Au}_{40}$  and those of samples loaded on CNT, GR and  $\text{SiO}_2$  supports.

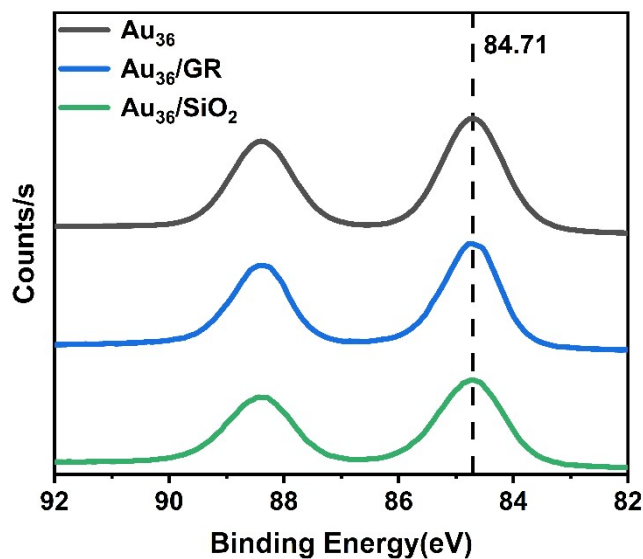


Fig. S22 XPS spectra of  $\text{Au}_{36}$  and those of samples loaded on CNT and GR.

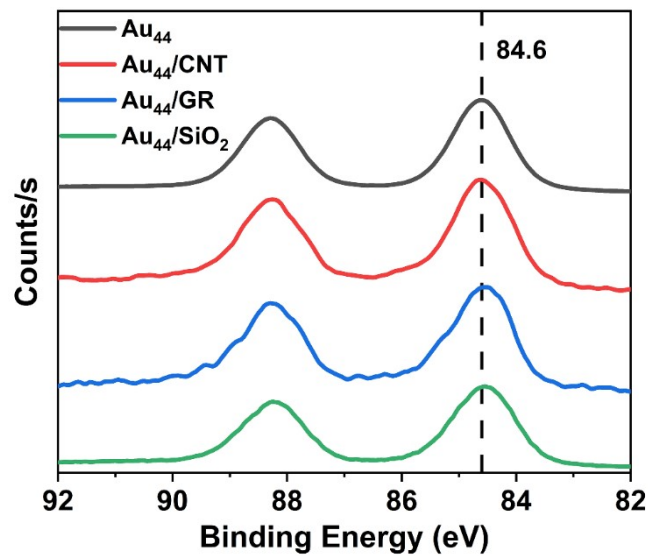


Fig. S23 XPS spectra of Au<sub>44</sub> and those of samples loaded on CNT, GR and SiO<sub>2</sub> supports.

## Reference

- 1 C. Zeng, Y. Chen, K. Iida, K. Nobusada, K. Kirschbaum, K. J. Lambright and R. Jin, *J. Am. Chem. Soc.*, 2016, **138**, 3950-3953.